Title

Wind-Induced Ground-Surface Pressures around a Single-Family House

Authors

Riley, W J
Gadgil, A J
Nazaroff, W W

Publication Date

1996-02-01

LBL-38435
UC-1600
Preprint

Lawrence Berkeley Laboratory

UNIVERSITY OF CALIFORNIA

ENERGY & ENVIRONMENT DIVISION

Accepted for publication in The Journal of Wind Engineering and Industrial Aerodynamics

Wind-Induced Ground-Surface Pressures around a Single-Family House

W.J. Riley, A.J. Gadgil, and W.W. Nazaroff

February 1996

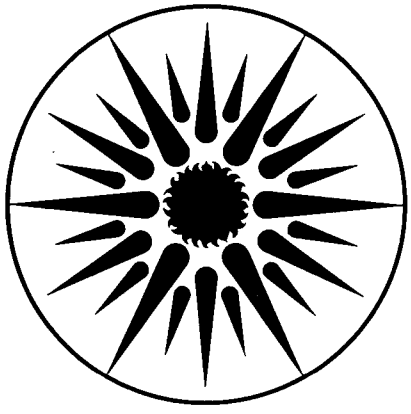

ENERGY AND ENVIRONMENT DIVISION

Prepared for the U.S. Department of Energy under Contract Number DE-AC03-76SF00098

DISCLAIMER

LBL-38435
UC-1600

Wind-Induced Ground-Surface Pressures around a Single-Family House

W.J. Riley,†‡ A.J. Gadgil,‡ W.W. Nazaroff†

†Department of Civil and Environmental Engineering
University of California, Berkeley

and

‡Indoor Environment Program
Energy and Environment Division
Ernest Orlando Lawrence Berkeley National Laboratory
University of California
Berkeley, California 94720

February 1996

This work was supported by the Assistant Secretary for Energy Efficiency and Renewable Energy, Office of Building Technologies, Building Systems and Materials Division, of the U.S. Department of Energy under Contract No. DE-AC03-76SF00098.

ABSTRACT

Wind induces a ground-surface pressure field around a building that can substantially affect the flow of soil gas and thereby the entry of radon and other soil-gas contaminants into the building. To quantify the effect of the wind-induced ground-surface pressure field on contaminant entry rates, the mean ground-surface pressure field was experimentally measured in a wind tunnel for several incidence angles of the wind, two atmospheric boundary layers, and two house geometries. The experimentally measured ground-surface pressure fields are compared with those predicted by a k-ε turbulence model. Despite the fundamental limitations in applying a k-ε model to a system with flow separation, predictions from the numerical simulations were good for the two wind incidence angles tested.

Key work index: wind-induced ground-surface pressures, soil-gas transport, radon entry, wind effects

NOMENCLATURE

$c_p(x,y)$	mean ground-surface pressure coefficient at (x,y) (-)
$c_p\|_{\mathrm{F}}(x,y)$	mean ground-surface pressure coefficient at (x,y), from FLUENT (-)
$c_p\|_{\mathrm{W}}(x,y)$	mean ground-surface pressure coefficient at(x,y), from the wind tunnel (-)
d	displacement height (m)
$E(x,y)$	error in predicted pressure coefficient at (x,y) (-)
$I(z)$	turbulence intensity (-)
K	von Karman's constant (0.4)
k	turbulent kinetic energy per unit mass of fluid ($m^2 s^{-2}$)
$p_{gs}(x,y)$	mean ground-surface pressure at (x,y) (Pa)
p_∞	free stream pressure (Pa)
$U(z)$	mean wind speed at height z ($m s^{-1}$)
U_{ref}	mean wind speed at stationary reference pitot tube ($m s^{-1}$)
u_*	friction velocity ($m s^{-1}$)
V_{eh}	mean wind speed at eave height ($m s^{-1}$)
(x,y)	ground-surface coordinates (m)
z_0	roughness length (m)
z	height above the ground surface (m)

Greek letters

ε	rate of dissipation of turbulent kinetic energy per unit fluid mass ($m^2 s^{-3}$)
ρ	air density ($kg m^{-3}$)
$\sigma(z)$	standard deviation of $U(z)$ at height z ($m s^{-1}$)
τ_0	shear stress at the ground surface ($kg m^{-1} s^{-2}$)

Introduction

The indoor environment is an important site for human exposure to airborne contaminants (Nero [1]). Indoor air contaminants can originate from many sources, including building materials, furnishings, consumer products, and the soil surrounding the house. The present work is aimed at developing a better understanding of the soil-gas transport and entry into houses of radon and volatile organic compounds (VOCs). In this context, wind is of interest because its interaction with the building structure and nearby soil surface can significantly affect soil-gas movement around, and into, the house.

Research on the entry of soil-gas contaminants into buildings is motivated by the relatively large risks associated with exposure to these compounds. The lifetime risk of lung cancer from exposure to average U.S. indoor radon concentrations is estimated to be 0.4% (EPA [2]). This risk is several orders of magnitude larger than the risks associated with many other environmental contaminants currently of concern. Carcinogenicity is also a concern for VOCs that can enter houses via pathways analogous to those of radon (Wallace [3], Little *et al.* [4]). Benzene, for example, is recognized as a human leukemogen (IARC [5]).

Our laboratory is engaged in an ongoing effort to develop models that characterize the environmental and building factors affecting indoor contaminant concentrations. The understanding gained from these models can be used to determine which parts of the population are at risk, to decide where resources should be spent, and to design efficient and effective mitigation systems.

The effects of wind on a building's ventilation rate and relative depressurization with respect to outdoor air have been thoroughly studied (e.g., Sherman [6], Ernest [7], Feustel and Sherman [8]). However, the wind-induced ground-surface pressure field has largely been ignored in models of contaminant entry into houses (Gadgil [9]). Several authors have presented empirical evidence indicating that this pressure field may be significant when determining radon entry rates (Turk *et al.* [10], Nazaroff *et al.* [11]). A related paper (Riley *et al.* [12]) investigates the effects of wind on radon entry and indoor radon concentrations. In that work, the wind tunnel data reported here are used as input to a three-dimensional numerical model of soil gas and radon transport. We demonstrate that ignoring the wind-induced ground-surface pressure field can lead to large errors in predicted soil gas and radon entry rates, especially in high-permeability soils.

Other authors have published wind tunnel studies of flow around bluff bodies that include measurement of the ground-surface pressure distribution. Sakamoto and Mikio [13] examined the flow around a cube in a turbulent boundary layer and presented contour plots of the pressure distribution on the ground surface. Unfortunately, the results correspond to cube heights that are relatively large compared to the boundary layer thickness, and therefore do not correspond to the case of a building immersed in the atmospheric boundary layer. The lowest ratio of cube height to boundary layer thickness for which they report results is 0.4, whereas typical values for the ratio of house height to boundary layer depth are less than 0.1. Surry [14] and Okada and Ha [15] present the ground-surface pressure coefficient at several positions around a test building at Texas Tech University. The coverage of these measurements, however, is insufficient for our purposes. Levitan [16] has performed a wind tunnel study and measurements of the ground-surface pressure field around this same building. Although the building geometry

is somewhat different than ours, the ground-surface pressure fields he reports are qualitatively similar to those we present here.

Scott [17] reported results, generated in a small wind tunnel, of the mean ground-surface pressure distribution around a single-family home. This information was then used to predict radon entry rates into a house during a summer and winter period in Toronto. In this paper we extend Scott's work by more carefully controlling the experimental conditions and investigating the feasibility of replacing the wind tunnel experiments with numerical simulations.

Because wind tunnel experiments are relatively expensive, numerical simulation of air flow around buildings has begun to receive considerable attention. There are many simulation techniques, broadly characterized by their treatment of turbulence, for modeling these flows. The simplest numerical simulation techniques applicable to the present problem are based on the k-ε turbulence model. In this model, the eddy viscosity is linked to the turbulent kinetic energy per unit fluid mass, k ($m^2\ s^{-2}$), and the rate of dissipation of turbulent kinetic energy per unit fluid mass, ε ($m^2\ s^{-3}$). The details of the k-ε model are thoroughly documented elsewhere (e.g., Anderson *et al.* [18]).

Generally, this modeling approach encounters difficulty predicting the flow separation that occurs in the vicinity of bluff bodies. Murakami [19] attributes this to an overestimate of the turbulent kinetic energy in the region of separation, which leads to an overestimate of the eddy viscosity. Nevertheless, the k-ε turbulence model has been used extensively to simulate the flow around buildings immersed in turbulent boundary layers. Patterson and Apelt [20] report very good agreement with experimental results for mean pressures in the vicinity of a cube. Stathopoulos and Zhou [21] studied wind flow around an L-shaped building. They concluded that their simulation results provided good prediction of building surface pressures, except at areas near the building edges when the wind incidence is oblique. In a full-scale building experiment, Hoxey and Richards [22] report a number of differences between the experimental measurements and model predictions of the pressure field, especially in regions of separated flow. However, they state that the overall structure of the pressure distribution is well described by the model. Zhang *et al.* [23] studied a cubic building and report that the computed mean velocity fields show good agreement with wind tunnel measurements; no results were presented for the pressure field around the body.

Current state-of-the-art techniques, such as large eddy simulations, are designed to predict the complex wind flows around buildings more accurately. The increase in accuracy possible with these models comes at the expense of a large increase in computation time (e.g., Ferziger [24], Murakami [19]). One goal of the present work, together with that reported in Riley *et al.* [12], is to test whether the relatively inexpensive k-ε turbulence model can provide sufficiently accurate ground-surface pressure fields for the simulation of soil-gas contaminant transport around houses.

Materials and Methods

Boundary Layer Wind Tunnel

The experiments were performed in the boundary-layer wind tunnel of the Department of Architecture at the University of California, Berkeley. A detailed description of the wind tunnel can be found in Bauman *et al.* [25]. The test area has a cross section of 1.5 m high by 2.1 m wide, and the house model can be oriented at any angle to the incident wind by means of a turntable. A scale of 1:61 was used for the experiments; however, all dimensions reported here will be full-scale values. Three pressure transducers were used to measure the distribution of mean ground-surface pressures around the model building and the free stream dynamic and static pressures. The wind speed was measured with a hot-wire anemometer at 60 elevations in the boundary layer. At each height, 30 readings per second were taken for 30 seconds. The mean and standard deviation of the wind speed were calculated from these data.

For an adiabatic atmosphere, and for the flow through the wind tunnel, the horizontal wind speed in the vicinity of the ground surface is often represented by a logarithmic profile (Seinfeld [26])

$$U(z) = \frac{u_*}{K} \ln\left(\frac{z - d}{z_0}\right) \tag{1}$$

where $U(z)$ is the mean horizontal wind speed (m s^{-1}) at height z (m), u_* is the friction velocity (m s^{-1}), K is von Karman's constant (0.4), z_0 is the roughness length (m), and d is the displacement height (m). The displacement height is the distance above the ground surface where $U(z)$ begins to follow the logarithmic profile. It is typically less than the average height of the surrounding buildings, and is taken to be zero for smooth surfaces. The friction velocity, u_*, is defined as $\sqrt{\frac{\tau_0}{\rho}}$, where τ_0 is the shear stress at the ground surface (kg m^{-1} s^{-2}) and ρ is the air density (kg m^{-3}).

The turbulence intensity, $I(z)$ (-), indicates the size of the velocity fluctuations with respect to the mean velocity

$$I(z) = \frac{\sigma(z)}{U(z)} \tag{2}$$

where $\sigma(z)$ is the standard deviation of $U(z)$.

Experiments were performed for two different atmospheric boundary layers. The first had a roughness length of 0.1 m and a displacement height of 0 m (referred to hereafter as the "countryside" boundary layer), corresponding to the outskirts of a small town or a countryside with many hedges, some trees, and some buildings (ESDU [27]). The second had a roughness length of 0.29 m and a displacement height of 6 m (referred to hereafter as the "suburban" boundary layer), corresponding to the suburbs of a large town or the interior of a small town. These values were chosen to bound the range of expected conditions around most single family homes. The boundary layers are

established in the wind tunnel by placing blocks on the floor upwind of the house model.

Figures 1 and 2 show the experimental and analytical profiles of horizontal wind speed and turbulence intensity for these two boundary layers. The analytical horizontal wind speed is calculated from equation (1) and the turbulence intensity profile is from ESDU [27]. The shear velocities used in the analytical curves are averages over the boundary layer depth: 0.35 m s^{-1} for the countryside boundary layer, and 0.48 m s^{-1} for the suburban boundary layer.

Model Geometry and Pressure Measurement

The house geometry used in the wind tunnel experiment was chosen to represent a typical single-family structure in size and aspect ratio. The building has a plan area of 8.7 m x 10.4 m, a height of 3 m, a 6:12 roof pitch (rise:run), and an eave overhang of 30 cm (Figure 3). The model blocks 0.2% of the wind-tunnel cross section. Separate experiments were performed with a gable roof and a flat roof to determine the effect of roof geometry on the ground-surface pressure field. The permeability of a building's walls (e.g., open windows) was not considered in either our wind tunnel or numerical modeling experiments. We expect that the error introduced by this simplification is small.

The data acquisition system in the wind tunnel can record 66 pressure measurements at discrete points without interrupting the experiment. The complete pressure field was determined by recording 66 values on half of the ground surface and then rotating the house 180° and recording another 66 values. Thus, mean ground-surface pressures were determined at 132 points around the house for each case. Experiments were run at eight wind angles (every 45°) for each boundary layer and house geometry. By taking advantage of symmetry, the data were combined into results for three incident wind angles: 0° (perpendicular to the short side of the house), 45°, and 90° (perpendicular to the long side of the house).

Pressures were read 30 times per second for 30 seconds at each tap location; the mean and standard deviation of the values were recorded. A delay of 15 seconds between measurements at successive pressure taps was imposed to dampen any fluctuations caused by switching between taps. The pressure transducers were calibrated using a manual micromanometer.

The mean ground-surface pressures were normalized with respect to the eave-height free-stream dynamic pressure to give the mean ground-surface pressure coefficient, $c_p(x,y)$

$$c_p(x,y) = \frac{p_{gs}(x,y) - p_\infty}{\frac{1}{2}\rho V_{eh}^{\ 2}} \tag{3}$$

where $p_{gs}(x,y)$ is the mean ground-surface pressure (Pa) at location (x,y), p_∞ is the mean free stream pressure (Pa), ρ is the air density (kg m^{-3}), and V_{eh} is the mean wind speed at eave height (m s^{-1}).

Numerical Simulations

FLUENT is a commercially available software package that models a wide range of fluid flow phenomena by solving the conservation equations for mass and momentum (FLUENT [28]). A control-volume based, finite-difference method is used to discretize the equations, and we chose the k-ε model to simulate turbulence. The SIMPLEC algorithm, developed by Patankar [29], provides the iteration framework used to converge to a solution of the pressure and velocity fields.

The above-ground portion of the one-story house is modeled as a rectangular prism with horizontal dimensions of 10.4 m x 8.7 m and a height of 3 m. The physical space is discretized into 100,000 control volumes, and includes open space a distance of six house dimensions from the building in both horizontal directions, and a vertical dimension of 61 m. The ground is modeled as a smooth surface. We have assumed that the house is isolated from other buildings and that the flow profile at the inlet to the space corresponds to the "countryside" boundary layer. FLUENT computes pressure and velocity data at each of the node points in the numerical space. We report normalized mean ground-surface pressures (see equation 3).

Results and Discussion

Experimental Wind Tunnel Results

Contour plots of experimentally measured mean ground-surface pressure coefficients are presented in Figures 4 and 5. Figure 4 shows the mean ground-surface pressure coefficient fields for the "countryside" boundary layer. Figure 5 shows the analogous information for the "suburban" boundary layer. The pressure coefficient fields are remarkably similar, although the flow is perturbed by the building slightly less in the "countryside" boundary layer. As a result, equivalent contour lines are closer to the building for this case, particularly in the immediate vicinity of the house. Patterson and Apelt [20], in their numerical study of flow past a cube, reached a similar conclusion regarding the pressures near the ground when the boundary layer is altered. Their results, though, showed more discrepancies than do ours.

The effect of the roof geometry on the pressure field is illustrated by comparing the results in the left and right columns of either Figure 4 or 5. As expected, the building with the gable roof causes a larger perturbation of the flow and extension of the ground-surface pressure field. Changing from the gable roof to the flat roof has a larger effect on the pressure field than changing the atmospheric boundary layer. A steeper roof, or protuberances on the house, would also change the ground-surface pressures. These factors could have as large an influence on the ground-surface pressure field as the structure of the boundary layer.

To put our results in perspective, we note that a pressure difference of a few pascals between the basement and soil surface is often sufficient to draw significant amounts of soil gas into the house. Figures 4 and 5 indicate that pressure coefficients ranging from about 0.4 to 1 are present on the ground surface near the building. The 50th and 95th percentile wind speeds over a period of 25 years in Spokane, Washington, are 3.6 and 8.3 m s^{-1}, respectively (NOAA [30]). We chose Spokane for this illustration because radon entry and mitigation have been investigated in several houses in the area (Turk *et al.* [10]). For a 3.6 m s^{-1} wind the corresponding mean ground-surface pressures

range from about 3.1 to 7.8 Pa; at 8.3 m s^{-1} the range is about 17 to 41 Pa. These pressures are large in the context of soil-gas transport. The wind-induced ground-surface pressure field can therefore be a significant factor influencing contaminant entry into houses.

Numerical Simulation Results

The mean ground-surface pressure coefficients calculated by FLUENT for wind incidence angles of 0° and 45° are shown in Figure 6. Figure 6 (b) corresponds to the same boundary layer and house geometry as the wind tunnel results in Figure 4 (f), and Figure 6 (a) corresponds to Figure 4 (e).

Comparison Between Wind Tunnel and Simulation Results

We define the modeling error, $E(x,y)$, as the difference between the predicted pressure coefficients from FLUENT and the wind tunnel

$$E(x,y) = c_p\big|_F(x,y) - c_p\big|_W(x,y) \tag{4}$$

where $c_p\big|_F(x,y)$ is the mean pressure coefficient at the ground-surface location (x,y) calculated by FLUENT (-), and $c_p\big|_W(x,y)$ is the mean pressure coefficient at (x,y) determined in the wind tunnel (-). Figure 7 shows a plot of the error for the cases presented in Figures 4 (f) and 6 (b): wind from the "countryside" boundary layer incident perpendicular to the short side of the house with a flat roof. The errors are similar when the wind is incident at 45° to the house.

The FLUENT predictions are fairly accurate at the front and rear of the house. Directly behind the house the simulation pressure coefficients are more negative than the corresponding experimental values. This feature reverses at about 2 m behind the house, where the numerical predictions are less negative than the experimental values. The experimental pressure field extends further from the sides of the building than the simulated pressure field. A similar observation was made by Hoxey and Richards [22] in their numerical simulations of a full-scale experiment. The worst agreement between our simulated and observed pressure coefficients occurs towards the front of either side of the house. This is the region near the ground surface where the flow separates from the building, a feature the k-ε turbulence model often fails to accurately capture. Figure 8 is a histogram showing the distribution of errors in the pressure coefficient, $E(x,y)$, for the same boundary layer and house geometry as in Figure 7. The mean and standard deviation of these errors are 0.12 and 0.033, respectively. The distribution of error for wind incident at 45° to the house is similar to that shown in Figure 8.

Conclusions

We have performed wind tunnel experiments to determine the mean ground-surface pressure field established around a single-family house in the presence of wind. Two atmospheric boundary layers and two house geometries were studied. The mean ground-surface pressure fields determined in the wind tunnel experiment were compared

to predictions from a k-ε turbulence model simulation. Although the k-ε model has fundamental limitations simulating systems with flow separation, predictions from the numerical simulations were good for the two wind incidence angles tested (0° and 45°).

Our numerical simulations of the flow of soil gas around a building (Riley *et al.* [12]) indicate that radon entry rates are relatively insensitive to errors in the ground-surface pressure field that are on the order of those presented in Figure 7. We therefore conclude that, for a simple house geometry, the k-ε turbulence model predicts mean ground-surface pressure fields that are sufficiently accurate to study the steady-state transport of soil gas and radon in the presence of steady wind. Because the wind-induced ground-surface pressures influence soil-gas contaminant entry to a large extent, transient winds and more complicated geometries (e.g. multiple houses, multi-story houses) continue to be of research interest.

Acknowledgments

The authors wish to thank Adil Sharag-Eldin for his help with the wind tunnel experiments, Fred Bauman for helpful conversations and his review of the manuscript, and Ken Revzan and Iain Walker for their review of the manuscript. This work was supported by the Assistant Secretary for Conservation and Renewable Energy, Office of Building Technologies, Building Systems and Materials Division and by the Director, Office of Energy, Office of Health and Environmental Research, Human Health and Assessments Division and Pollutant Characterization and Safety Research Division of the U.S. Department of Energy under Contract No. DE-AC03-76SF00098. Additional support was provided by the National Science Foundation through grant BCS-9057298. A software license grant from FLUENT Inc. helped support the computational aspects of the work.

References

[1] Nero, A.V., Controlling indoor air pollution, Scientific American, 258 (5), 42-48, 1988.

[2] EPA, Technical Support Document for the 1992 Citizen's Guide to Radon, U.S. Environmental Protection Agency, EPA 400-R-92-011, 1992.

[3] Wallace, L.A., Comparison of risks from outdoor and indoor exposure to toxic chemicals, Environmental Health Perspectives, 95, 7-13, 1991.

[4] Little, J.C., J.M. Daisey and W.W. Nazaroff, Transport of subsurface contaminants into buildings, Environmental Science and Technology, 26, 2058-2066, 1992.

[5] IARC, Evaluation of the carcinogenic risk of chemicals to humans. IARC Monograph No. 219. International Agency for Research on Cancer, Lyon, France, 1982.

[6] Sherman, M.H., Simplified modeling for infiltration and radon entry, LBL-31305, Lawrence Berkeley Laboratory, Berkeley, CA, USA, 1992.

[7] Ernest, D., Predicting wind-induced indoor air motion, occupant comfort, and cooling loads in naturally ventilated buildings, Ph.D. Dissertation, Department of Architecture, University of California Berkeley, 261, 1991.

[8] Feustel, H.E. and M.H. Sherman, A simplified model for predicting air flow in multizone structures, Energy and Buildings, 13, 217-230, 1989.

[9] Gadgil, A.J., Models of radon entry, Radiation Protection Dosimetry, 45, 373-380, 1992.

[10] Turk, B.H., R.J. Prill, D.T. Grimsrud, B.A. Moed and R.G. Sextro, Characterizing the occurrence, sources, and variability of radon in Pacific northwest homes, Journal of Air Waste Management Association, 40, 498-506, 1990.

[11] Nazaroff, W.W., H. Feustel, A.V. Nero, K.L. Revzan and D.T. Grimsrud, Radon transport into a detached one-story house with a basement, Atmospheric Environment, 19, 31-46, 1985.

[12] Riley, W.J., A.J. Gadgil, Y.C. Bonnefous and W.W. Nazaroff, The effect of steady winds on Rn-222 entry from soil into houses, accepted in Atmospheric Environment, 1995.

[13] Sakamoto, H. and A. Mikio, Flow around a cubic body immersed in a turbulent boundary layer, Journal of Wind Engineering and Industrial Aerodynamics, 9, 275-293, 1982.

[14] Surry, D., Pressure measurements on the Texas Tech building - wind tunnel measurements and comparisons with full scale, Journal of Wind Engineering Industrial Aerodynamics, 38, 235-247, 1991.

[15] Okada, H. and YC. Ha, Comparison of wind tunnel and full-scale pressure measurement tests on the Texas Tech building, Journal of Wind Engineering and Industrial Aerodynamics, 43, 1601-1612, 1992.

[16] Levitan, M.L., Analysis of reference pressure systems used in field measurements of wind loads, Ph.D. dissertation, Texas Tech University, Lubbock, Texas, 57-64, 1993.

[17] Scott, A.G., A computer model study of soil gas movement into buildings, Ottawa, Ontario, Canada, Department of Health and Welfare, Report No. 1389/1333, 1985.

[18] Anderson, D.A., J.C. Tannehill and R.H. Pletcher, Computational Fluid Mechanics and Heat Transfer, McGraw-Hill, New York, 1984.

[19] Murakami, S., Comparison of various turbulence models applied to a bluff body, Journal of Wind Engineering Industrial Aerodynamics, 46 & 47, 21-36, 1993.

[20] Patterson, D.A. and C.J. Apelt, Simulation of flow past a cube in a turbulent boundary layer, Journal of Wind Engineering and Industrial Aerodynamics, 35, 149-176, 1990.

[21] Stathopoulos, T. and Y.S. Zhou, Numerical simulation of wind-induced pressures on buildings of various geometries, Journal of Wind Engineering and Industrial Aerodynamics, 46 & 47, 419-430, 1993.

[22] Hoxey, R.P. and P.J. Richards, Flow patterns and pressure field around a full-scale building, Journal of Wind Engineering and Industrial Aerodynamics, 50, 203-212, 1993.

[23] Zhang, Y.Q., A.H. Huber, S.P.S. Arya and W.H. Snyder, Numerical simulation to determine the effects of incident wind shear and turbulence level on the flow around a building, Journal of Wind Engineering and Industrial Aerodynamics, 46 & 47, 129-134, 1993.

[24] Ferziger, J., Simulation of complex turbulent flows: Recent advances and prospects in wind engineering, Journal of Wind Engineering and Industrial Aerodynamics, 46 & 47, 195-212, 1993.

[25] Bauman, F.S., D.R. Ernest and E.A. Arens, ASEAN natural ventilation study: Wind pressure distributions on long building rows in urban surroundings, CEDR-03-88, Center for Environmental Design Research, University of California, Berkeley, CA, USA, 1988.

[26] Seinfeld, J.H., Atmospheric Chemistry and Physics of Air Pollution, John Wiley, New York, 494, 1986.

[27] ESDU, Engineering Sciences Data Unit, Characteristics of atmospheric turbulence near the ground, Part II, Item Number 85020, London, England, 1985.

[28] FLUENT, v4.2, Fluent Incorporated, Centerra Resource Park, 10 Cavendish Court, Lebanon, NH, 1993.

[29] Patankar, S.V., Numerical Heat Transfer and Fluid Flow, Hemisphere Publishing, 1980.

[30] NOAA, National Oceanic and Atmospheric Administration, Local climatological data, annual summaries for 1980, Part II - NEB-WYO, National Climatic Center, Asheville, NC 28801, 1980.

Figure 1. Experimental (•) and analytical (—) horizontal wind velocity (a), and turbulence intensity (b), as a function of height above the ground for the "countryside" boundary layer (z_0 = 0.10 m, d = 0 m). The solid line in (a) was calculated with equation (1) and in (b) from ESDU [27] correlations.

Figure 2. Experimental (•) and analytical (—) horizontal wind velocity (a), and turbulence intensity (b), as a function of height above the ground for the "suburban" boundary layer (z_0 = 0.29 m, d = 6 m). The solid line in (a) was calculated with equation (1) and in (b) from ESDU [27] correlations.

Figure 3. The wind tunnel building geometry (1:61 geometrical scale).

Figure 4. Wind tunnel mean ground-surface pressure coefficients for the "countryside" boundary layer (z_0 = 0.10 m, d = 0 m). Shown are results for the house with a gable and flat roof at three incident wind angles. The contour interval is 0.20.

Figure 5. Wind tunnel mean ground-surface pressure coefficients for the "suburban" boundary layer (z_0 = 0.29 m, d = 6 m). Shown are results for the house with a gable and flat roof at three incident wind angles. The contour interval is 0.20.

Figure 6. Numerical simulation mean ground-surface pressure coefficients for the "countryside" boundary layer (z_0 = 0.10 m, d = 0 m). Shown are results for the house with a flat roof at two incident wind angles. The contour interval is 0.20.

Figure 7. Contour plot of the error (numerical simulation value minus wind tunnel value) in mean ground-surface pressure coefficient for the "countryside" boundary layer (z_0 = 0.10 m, d = 0 m) incident perpendicular to the 8.7 m side of the house. The contour interval is 0.1.

Figure 8. Distribution of error (numerical simulation value minus wind tunnel value, equation 4) in mean ground-surface pressure coefficient for the "countryside" boundary layer (z_0 = 0.10 m, d = 0 m) incident perpendicular to the 8.7 m side of the house.

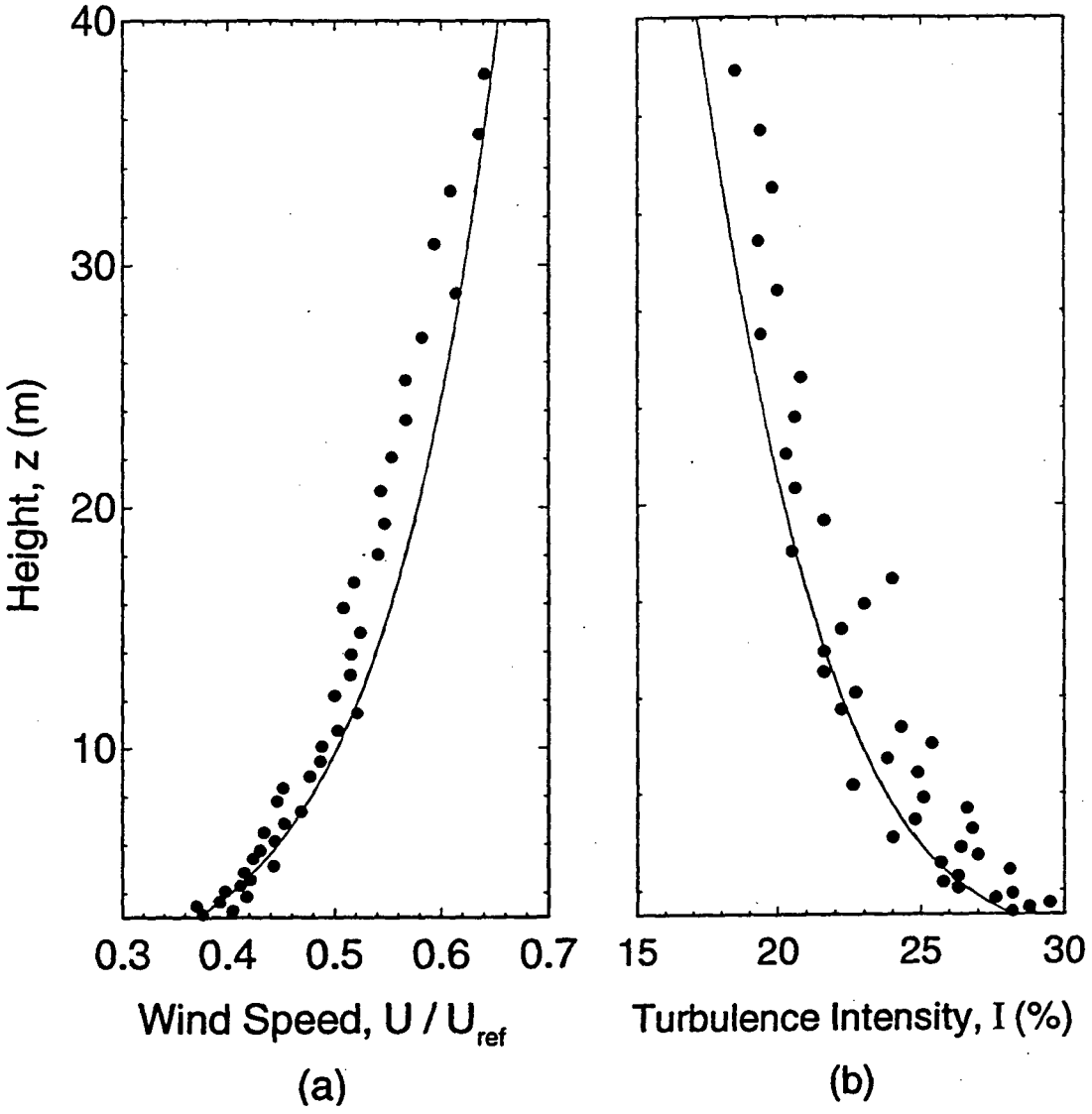

Figure 1. Experimental (•) and analytical (—) horizontal wind velocity (a), and turbulence intensity (b), as a function of height above the ground for the "countryside" boundary layer (z_0 = 0.10 m, d = 0 m). The solid line in (a) was calculated with equation (1) and in (b) from ESDU [27] correlations.

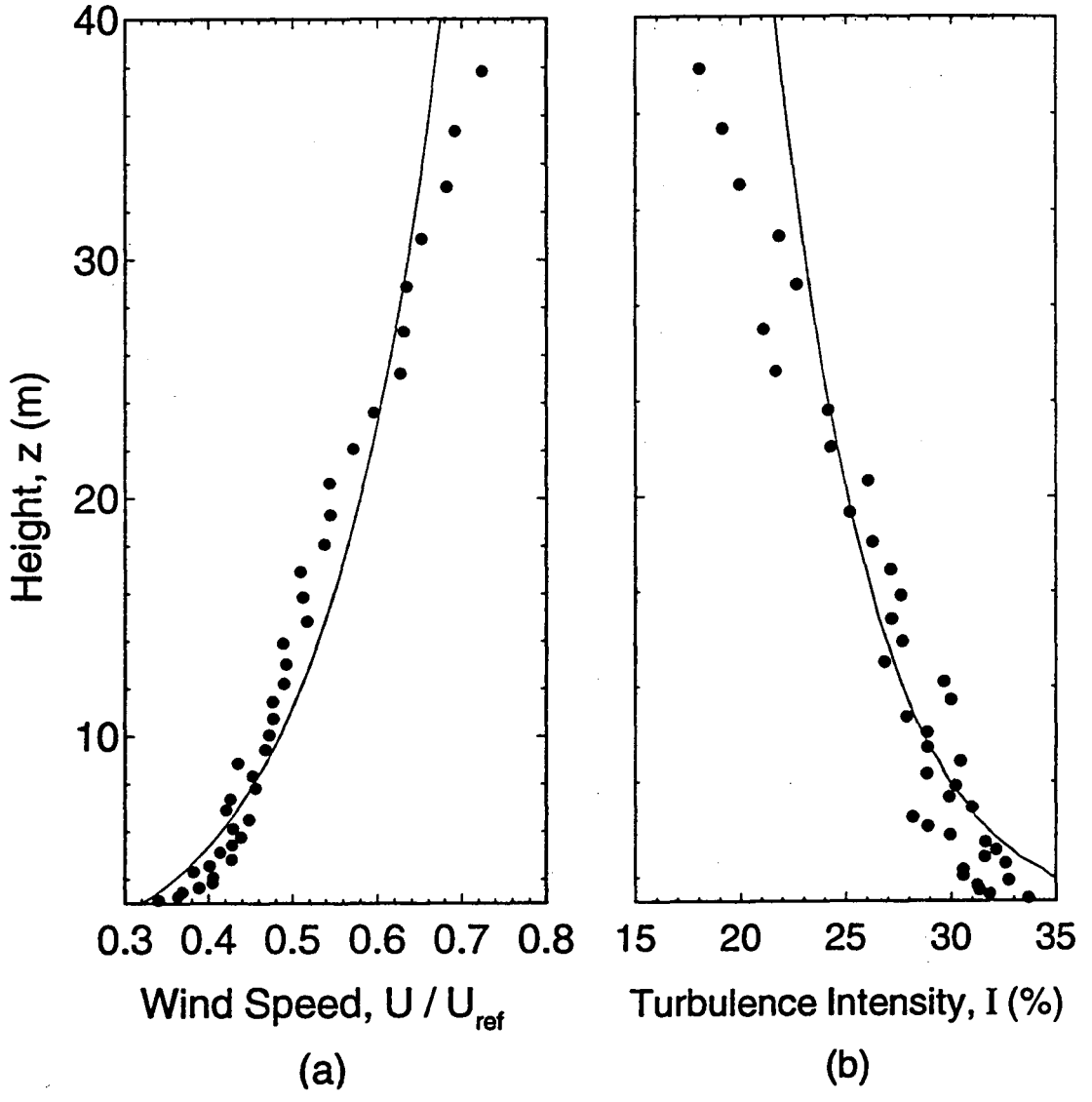

Figure 2. Experimental (•) and analytical (—) horizontal wind velocity (a), and turbulence intensity (b), as a function of height above the ground for the "suburban" boundary layer ($z_0 = 0.29$ m, $d = 6$ m). The solid line in (a) was calculated with equation (1) and in (b) from ESDU [27] correlations.

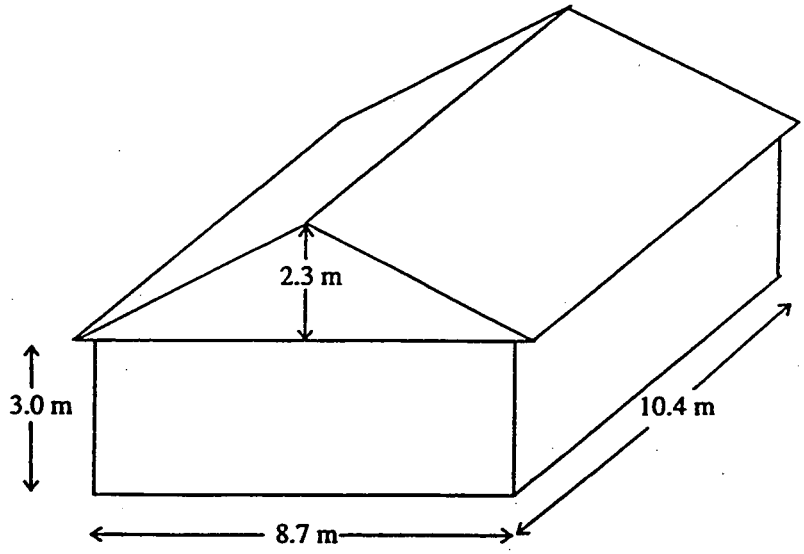

Figure 3. The wind tunnel building geometry (1:61 geometrical scale). The sketch is not to scale.

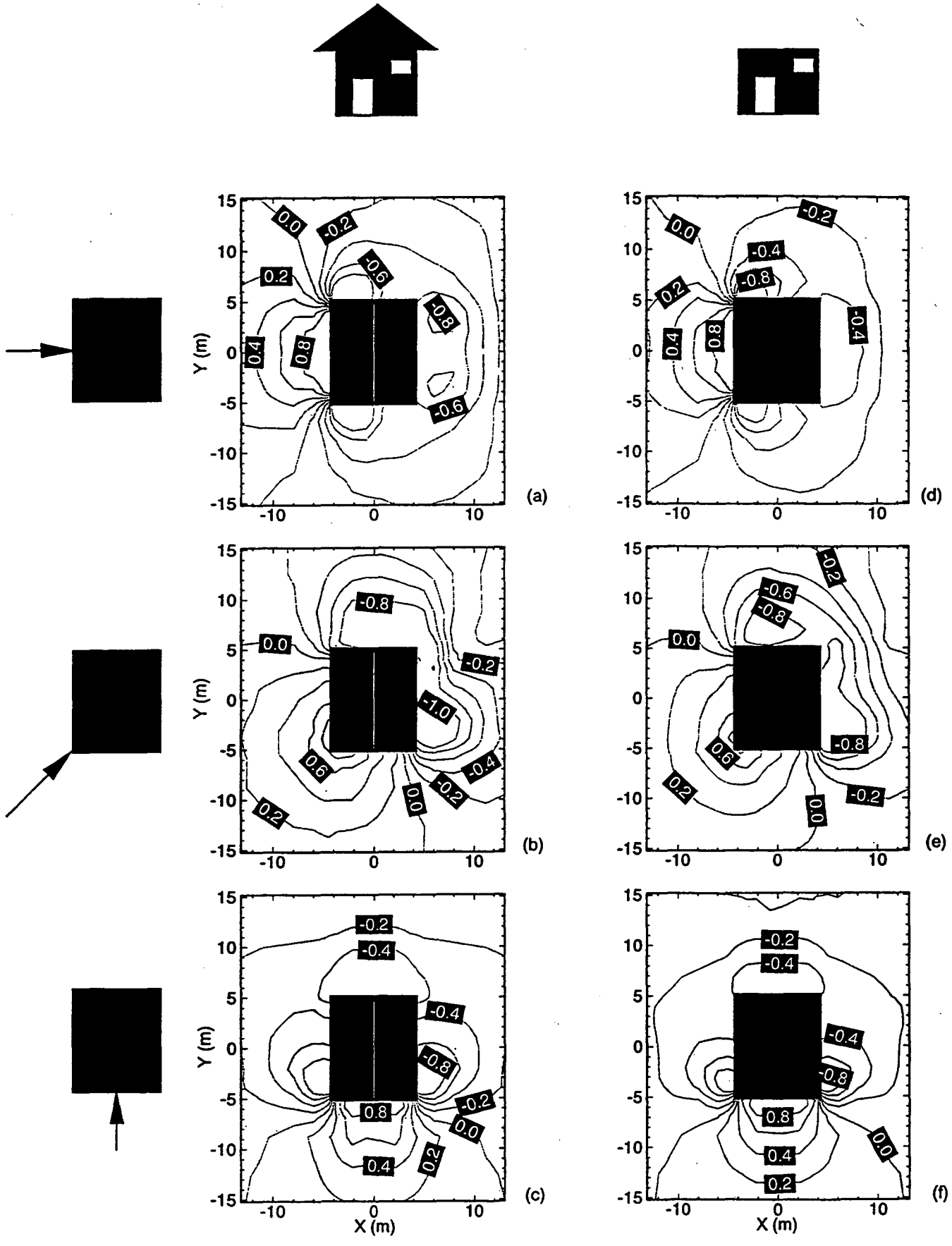

Figure 4. Wind tunnel mean ground-surface pressure coefficients for the "countryside" boundary layer (z_0 = 0.10 m, d = 0 m). Shown are results for the house with a gable and flat roof at three incident wind angles. The contour interval is 0.20.

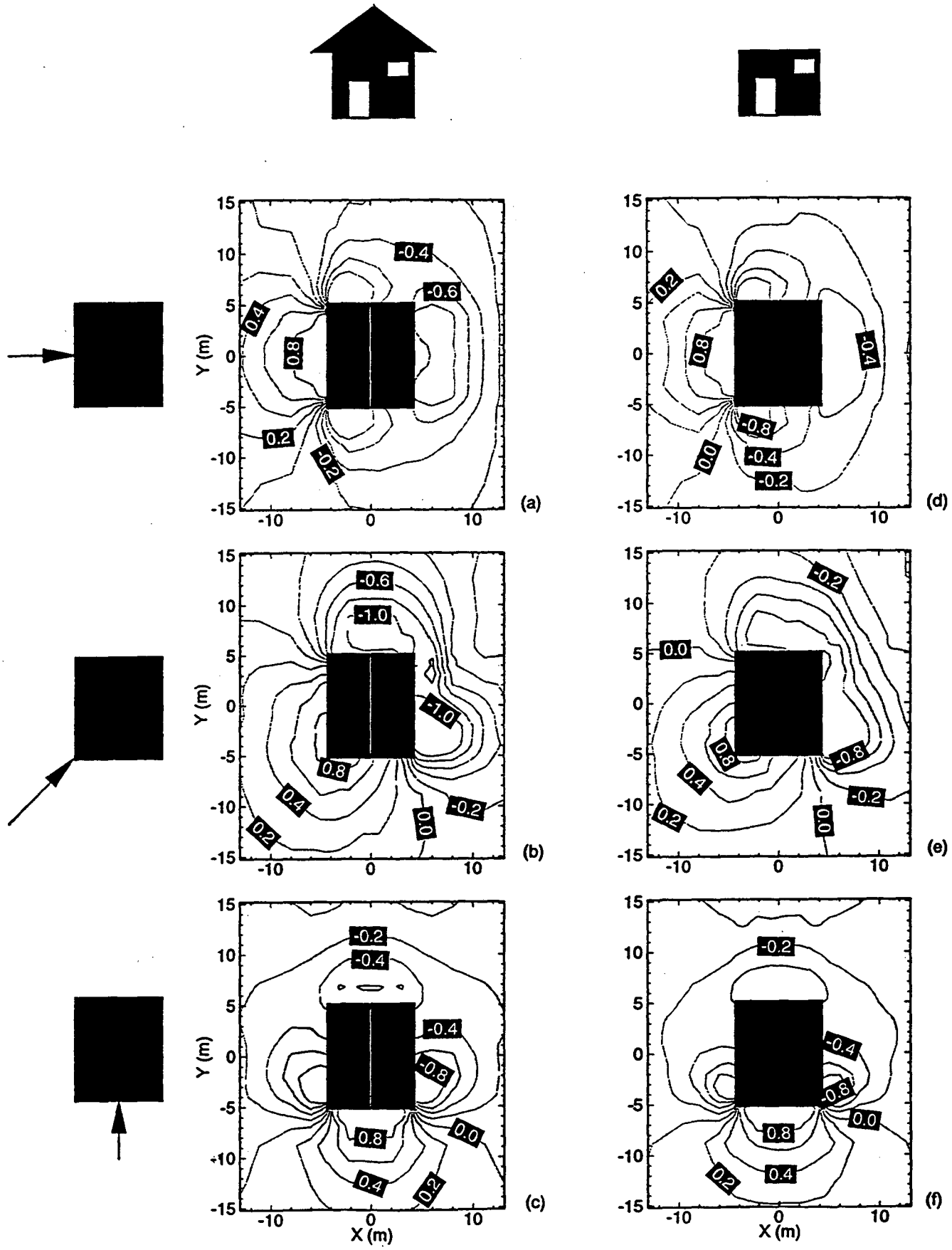

Figure 5. Wind tunnel mean ground-surface pressure coefficients for the "suburban" boundary layer (z_0 = 0.29 m, d = 6 m). Shown are results for the house with a gable and flat roof at three incident wind angles. The contour interval is 0.20.

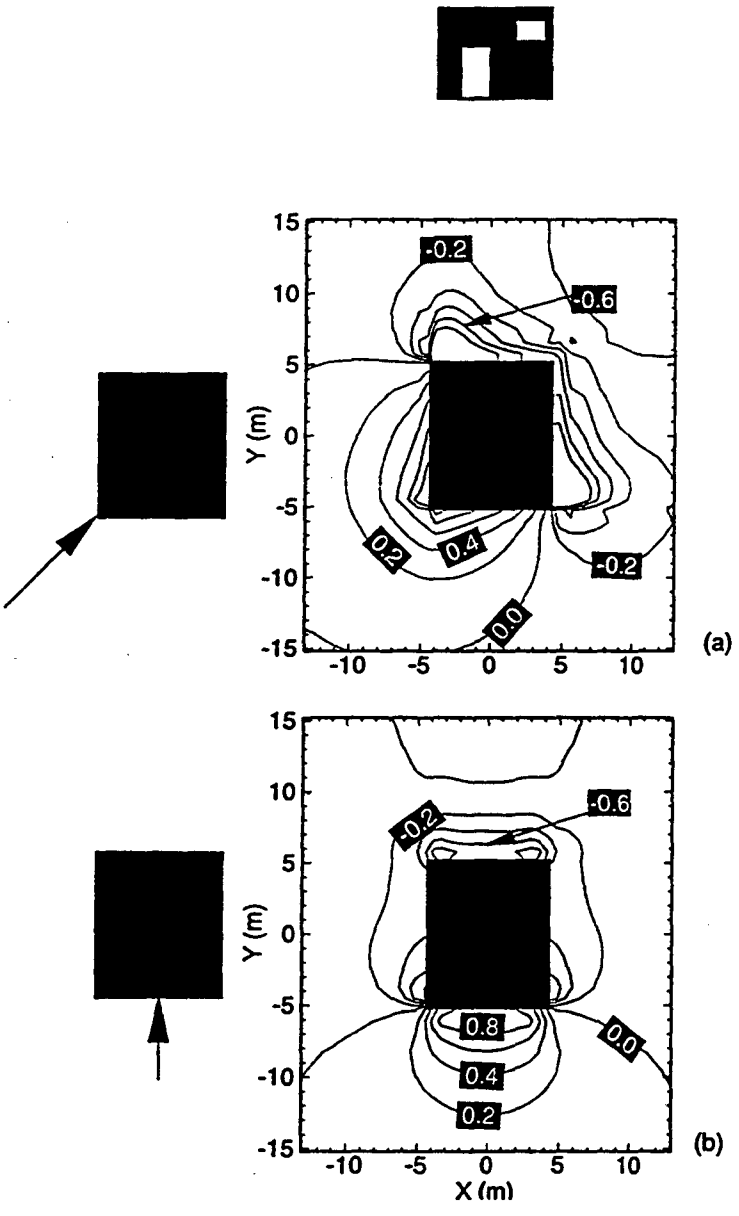

Figure 6. Numerical simulation mean ground-surface pressure coefficients for the "countryside" boundary layer (z_0 = 0.10 m, d = 0 m). Shown are results for the house with a flat roof at two incident wind angles. The contour interval is 0.20.

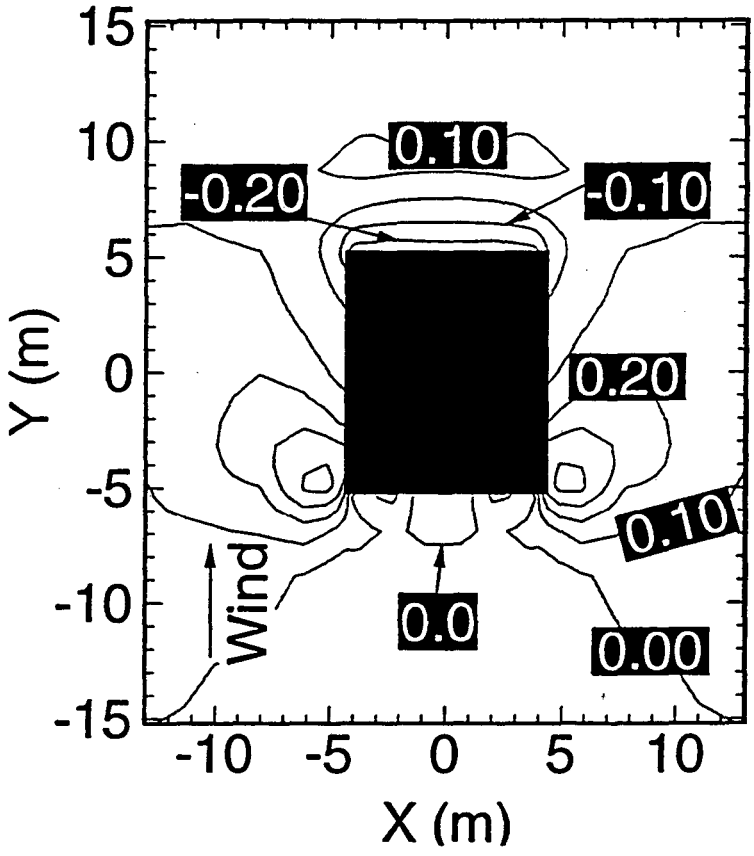

Figure 7. Contour plot of the error (numerical simulation value minus wind tunnel value) in mean ground-surface pressure coefficient for the "countryside" boundary layer (z_0 = 0.10 m, d = 0 m) incident perpendicular to the 8.7 m side of the house. The contour interval is 0.1.

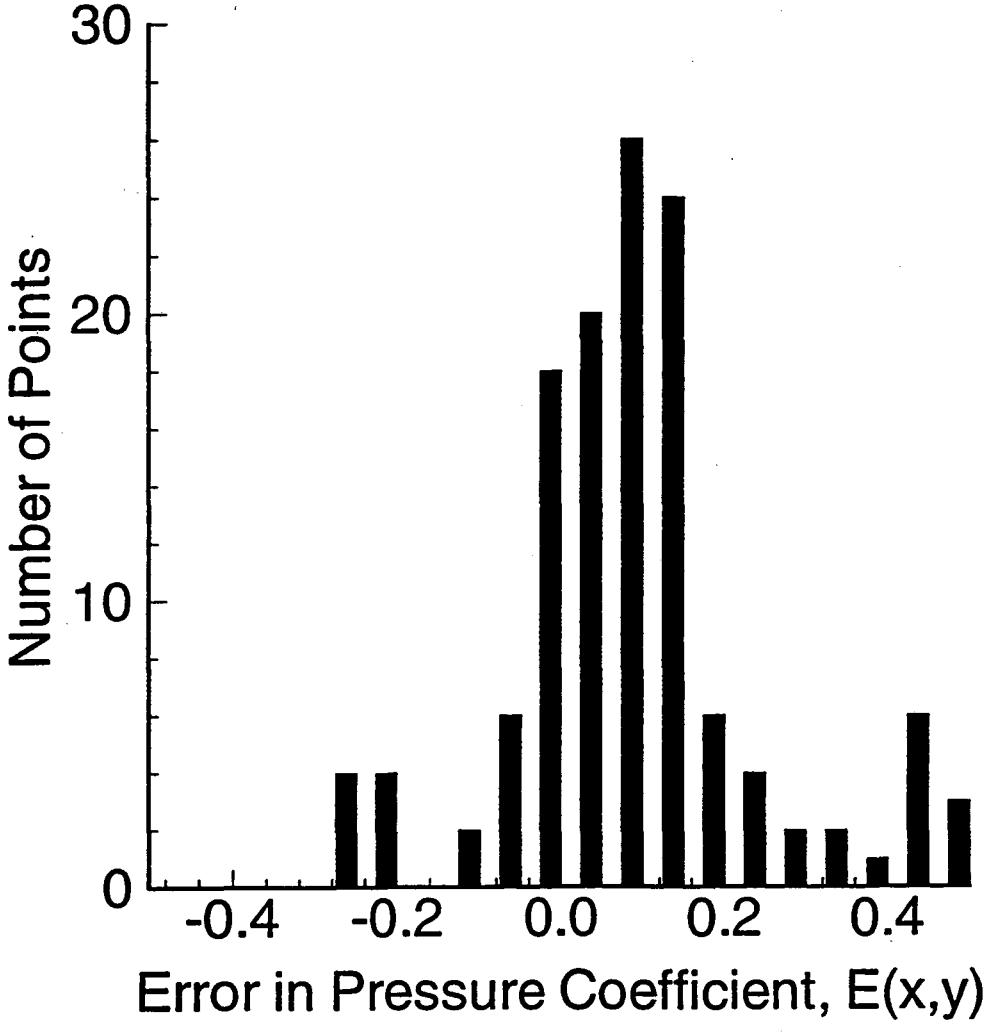

Figure 8. Distribution of error (numerical simulation value minus wind tunnel value, equation 4) in mean ground-surface pressure coefficient for the "countryside" boundary layer (z_0 = 0.10 m, d = 0 m) incident perpendicular to the 8.7 m side of the house.

LAWRENCE BERKELEY NATIONAL LABORATORY
UNIVERSITY OF CALIFORNIA
TECHNICAL & ELECTRONIC INFORMATION DEPARTMENT
BERKELEY, CALIFORNIA 94720